

RESEARCH ARTICLE

# High-level production and purification in a functional state of an extrasynaptic gamma-aminobutyric acid type A receptor containing $\alpha 4\beta 3\delta$ subunits

Xiaojuan Zhou, Rooma Desai, Yinghui Zhang, Wojciech J. Stec, Keith W. Miller\*, Youssef Jounaidi

Department of Anesthesia, Critical Care and Pain Medicine, Massachusetts General Hospital, Harvard Medical School, Boston, Massachusetts, United States of America

\* [kwmiller@mgh.harvard.edu](mailto:kwmiller@mgh.harvard.edu)



**OPEN ACCESS**

**Citation:** Zhou X, Desai R, Zhang Y, Stec WJ, Miller KW, Jounaidi Y (2018) High-level production and purification in a functional state of an extrasynaptic gamma-aminobutyric acid type A receptor containing  $\alpha 4\beta 3\delta$  subunits. PLoS ONE 13(1): e0191583. <https://doi.org/10.1371/journal.pone.0191583>

**Editor:** Uwe Rudolph, McLean Hospital/ Harvard Medical School, UNITED STATES

**Received:** August 15, 2017

**Accepted:** January 8, 2018

**Published:** January 19, 2018

**Copyright:** © 2018 Zhou et al. This is an open access article distributed under the terms of the [Creative Commons Attribution License](https://creativecommons.org/licenses/by/4.0/), which permits unrestricted use, distribution, and reproduction in any medium, provided the original author and source are credited.

**Data Availability Statement:** All relevant data are within the paper and its Supporting Information files.

**Funding:** This research was supported by grants from the National Institute of General Medical Sciences GM 58448 (to KWM) and by the Department of Anesthesia, Critical Care & Pain Medicine, Massachusetts General Hospital (to YJ, RD and KWM). The funders had no role in study

## Abstract

The inhibitory  $\gamma$ -aminobutyric acid type A receptors are implicated in numerous physiological processes, including cognition and inhibition of neurotransmission, rendering them important molecular targets for many classes of drugs. Functionally, the entire GABA<sub>A</sub>R family of receptors can be subdivided into phasic, fast acting synaptic receptors, composed of  $\alpha$ -,  $\beta$ - and  $\gamma$ -subunits, and tonic extrasynaptic receptors, many of which contain the  $\delta$ -subunit in addition to  $\alpha$ - and  $\beta$ -subunits. Whereas the subunit arrangement of the former group is agreed upon, that of the  $\alpha\beta\delta$  GABA<sub>A</sub>Rs remains unresolved by electrophysiological and pharmacological research. To resolve such issues will require biophysical techniques that demand quantities of receptor that have been previously unavailable. Therefore, we have engineered a stable cell line with tetracycline inducible expression of human  $\alpha 4$ -,  $\beta 3$ - and N-terminally Flag-tagged  $\delta$ -subunits. This cell line achieved a specific activity between 15 and 20 pmol [<sup>3</sup>H]muscimol sites/mg of membrane protein, making it possible to obtain 1 nmole of purified  $\alpha 4\beta 3\delta$  GABA<sub>A</sub>R from sixty 15-cm culture dishes. When induced, these cells exhibited agonist-induced currents with characteristics comparable to those previously reported for this receptor and a pharmacology that included strong modulation by etomidate and the  $\delta$ -subunit-specific ligand, DS2. Immunoaffinity purification and reconstitution in CHAPS/asolectin micelles resulted in the retention of equilibrium allosteric interactions between the separate agonist, anesthetic and DS2 sites. Moreover, all three subunits retained glycosylation. The establishment of this well-characterized cell line will allow molecular level studies of tonic receptors to be undertaken.

## Introduction

GABA<sub>A</sub>Rs, which are members of the Cys-loop pentameric ligand-gated ion channel superfamily, are the main inhibitory neuroreceptors in the brain and the target of many drugs and

design, data collection and analysis, decision to publish, or preparation of the manuscript.

**Competing interests:** The authors have declared that no competing interests exist.

endogenous ligands. Most naturally occurring GABA<sub>A</sub>Rs are heteropentamers made up from the 19 known highly homologous subunits (for a review see Olsen and Sieghart (1)). The functional properties of GABA<sub>A</sub>Rs depend on their subunit composition. Two important classes of GABA<sub>A</sub>R in the brain are the synaptic receptors that all contain  $\alpha\beta\gamma$  subunits and the extra-synaptic receptors that often contain  $\alpha\beta\delta$  subunits [1]. These receptors mediate phasic and tonic currents respectively (reviewed in [2, 3]). The agonist GABA activates tonic receptors at lower concentrations and with lower efficacy than phasic receptors. The tonic receptors are of great significance, being thought to be involved in sleep, stress, psychiatric disorders, epilepsy, learning, memory and neuroprotection [3].

Because positive allosteric effectors act in interfaces between subunits, the variable composition and arrangement of each GABA<sub>A</sub>R's subunits provides opportunities for the development of drugs that bind selectively to different receptor subtypes [4, 5]. For example, the synaptic receptors are targeted by benzodiazepines that bind between  $\alpha$ - and  $\gamma$ -subunits in the extracellular domain, whereas the general anesthetic etomidate acts on tonic and phasic receptors by binding between  $\beta$  (except  $\beta 1$ ) and  $\alpha 1$ – $6$  subunits in the transmembrane domain. With the exception of DS2 and its analogs, which selectively modulate tonic  $\delta$ -subunit containing GABA<sub>A</sub>Rs, no other drugs specific to those receptors have been developed [6].

Whilst phasic receptors are commonly agreed to be arranged  $\beta$ – $\alpha$ – $\beta$ – $\alpha$ – $\gamma$ , there is considerable uncertainty surrounding the stoichiometry and arrangement of the  $\alpha$ -,  $\beta$ - and  $\delta$ -subunits in tonic receptors. Electrophysiological studies in oocytes suggest that several arrangements are possible depending on the ratio of constructs transfected [7, 8]. However, the properties of these receptors depend on the expression system, and it has been reported that expression in HEK cells leads to less variability with the most likely arrangement being  $\beta 2$ – $\alpha 4$ – $\beta 2$ – $\alpha 4$ – $\delta$  [9]. On the other hand, even in HEK cells the subunit stoichiometry depends on the ratio of the constructs used in transfection; titration of construct ratios in  $\alpha 1\beta 2\delta$  receptors in HEK cells led to the conclusion that several subunit arrangements are possible [10]. In a thorough quantitative Western blotting study of  $\alpha 4\beta 2\delta$  receptors in which subunit transfection ratios were varied, it was concluded that the amount of the  $\delta$ -construct transfected correlated with the  $\delta$ -subunit incorporated into the pentamer at the expense of the  $\beta 2$ -subunit [11].

Given the above issues, we sought to develop a stable cell line that expressed large quantities of tonic  $\alpha 4\beta 3\delta$  GABA<sub>A</sub>Rs. The advantages of such a high yielding cell line would include the ability to study gating in receptors with low open probability ( $P_{open}$ ) and to undertake biophysical and structural studies in purified, reconstituted receptors. Here, extending our previous work on  $\alpha 1\beta 3$  and synaptic  $\alpha 1\beta 3\gamma 2$  GABA<sub>A</sub>Rs [12, 13], we report the high-level expression, electrophysiological characterization, purification, and functional reconstitution into CHAPS/asolectin micelles of human extrasynaptic  $\alpha 4\beta 3\delta$  GABA<sub>A</sub>Rs using an inducible HEK293-TetR cell line [14].

## Materials and methods

### Cloning of $\alpha 4$ and $\delta$ subunits

A human brain cDNA library (Clontech, Mountain View, CA) was used to clone the cDNAs of GABA<sub>A</sub> receptor  $\alpha 4$ - and  $\delta$ -subunits. A 1665 bp cDNA fragment corresponding to 984–2650 base pairs of  $\alpha 4$ -subunit (GenBank Accession # NM\_000809) and a 1359 bp cDNA corresponding to 96–1454 base pairs of  $\delta$ -subunit (GenBank Accession # NM\_000815) were amplified by PCR using DNA polymerase *Pfu* ultra (Agilent Technologies, Santa Clara, CA). The sequences of PCR primers used are specified in S1 Table. The human  $\beta 3$  (NM\_021912.3) cDNA was cloned previously [12]. The cDNAs of  $\alpha 4$ ,  $\beta 3$ , and  $\delta$ -subunits were sub-cloned into different tetracycline-inducible, mammalian expression vectors that conferred resistance to

different drugs. The  $\alpha 4$ -subunit was sub-cloned into pCDNA4/TO (zeocin; Life Technologies, Grand Island, NY), the  $\beta 3$ -subunit into pCDNA3.1/TO (hygromycin; Life Technologies) and the  $\delta$ -subunit into pACMV/TetO (G418/geneticin, Life Technologies). The estimated molecular weight of each genetic construct is  $4.43 \times 10^6$  g/mol for  $\alpha 4$ -subunit,  $4.59 \times 10^6$  g/mol for  $\beta 3$ -subunit and  $5.86 \times 10^6$  g/mol for  $\delta$ -subunit. Sanger DNA sequencing at MGH DNA core was used to confirm the DNA sequences of all three GABA<sub>A</sub>R subunits.

### **Pfu Mutagenesis to insert Flag-tag in human GABA<sub>A</sub>R $\delta$ -subunit**

SignalP 4.1 server (<http://www.cbs.dtu.dk/services/SignalP>) was used to predict the signal sequence in the  $\alpha 4$ - and  $\delta$ -subunit protein sequences [15]. A Flag-tag, DYKDDDDK, was inserted between amino acid 4 and 5 of the predicted mature  $\alpha 4$ -subunit and amino acids 5 and 6 of the  $\delta$ -subunit protein by Pfu mutagenesis using DNA polymerase *Pfu* ultra (Agilent Technologies), as outlined in the S1 Text. The respective  $\delta$ -subunit-pACMV/TetO or  $\alpha 4$ -subunit-pCDNA4/TO plasmids generated were used as reaction templates. The sequence of the primers used for mutagenesis is specified in S1 Table. Sanger DNA sequencing at MGH DNA core facility confirmed insertion of the Flag-tag at desired locations.

### **Transfection protocol**

HEK293-TetR cells [14, 16] expressing the tetracycline repressor protein (TetR) were cultured in DMEM/F12 (Life Technologies, Grand Island, NY) supplemented with 10% fetal bovine serum (Atlanta Biologicals, Flowery Branch, GA), 5  $\mu$ g/ml Blasticidin (Lifesciences), 0.2% penicillin/streptomycin (Life Technologies) at 37°C with 5% CO<sub>2</sub>. Cells seeded at a density of 250,000 cells/well in a 6-well plate were allowed to settle for 24h and transfected with a total of 4  $\mu$ g DNA using Lipofectamine 2000 (Life Technologies), according to manufacturer instructions. Cells expressing N-Flag- $\alpha 4\beta 3$  were transfected with DNA constructs at the weight ratio of 2:1 ( $\alpha 4$ : $\beta 3$ , respectively), whilst  $\alpha 4\beta 3$ N-Flag- $\delta$  receptor was prepared with 2:1:0.25 ( $\alpha 4$ : $\beta 3$ : $\delta$ , respectively). To select for drug resistant cells, after 48 hours, the growth medium was supplemented with 250  $\mu$ g/ml zeocin and 50  $\mu$ g/ml hygromycin for the N-Flag- $\alpha 4\beta 3$  expressing line and additionally with 200  $\mu$ g/ml G418 for the  $\alpha 4\beta 3$ N-Flag- $\delta$  expressing line for the selection of drug resistant cells. Cells were maintained in medium with antibiotics.

### **Stabilization of cell lines**

Exponentially growing drug-resistant cells were harvested and resuspended in PBS supplemented with 3% FBS. N-Flag- $\delta$  or N-Flag- $\alpha 4$  subunit expression at the cell surface was detected using an anti-Flag M2 (Mouse anti-DYKDDDDK IgG (Clone M2), which binds the Flag epitope in any position) conjugated to SureLight<sup>®</sup> APC, Columbia Biosciences, Frederic, MD). Cells were sorted at MGH Flow Cytometry Core facility using a BD 5 laser SORP FACS Vantage SE Diva system (BD Biosciences, San Jose, CA) using argon-ion laser excitation (633 nm, 35 mW). Emission for APC was detected at 650 nm. Dead cells and debris were excluded from the analysis by gating for intact cells using the forward and sideways scatter (488 nm, 320 mW). Uninduced cells were included as a negative control for autofluorescence. Data acquisition was carried out by analyzing 10 000 events/sample using CellQuest Software (BD Biosciences). FACS data were analyzed using FlowJo Software (Tree Star).

Following resorting of the cells in the pool in S1B Fig, one cell per well was seeded in a 96-well plate and cultured in antibiotic-enriched media. Some two dozen of these clones were analyzed for expression using flow cytometry and then by [<sup>3</sup>H]muscimol binding. The flow cytometry profile of the clone finally selected is shown in S1C & S1D Fig.

## Radioactive ligand binding

Radioactive ligand binding assays were carried out as previously described [13], with the exception that GABA<sub>A</sub>R binding sites were assayed at 250 nM [<sup>3</sup>H]muscimol because of this receptor's higher affinity.

## Preparation of membrane, solubilization, immunoaffinity purification and reconstitution into CHAPS/asolectin micelles of receptors

Cells with inducible expression of N-Flag- $\alpha 4\beta 3$  and  $\alpha 4\beta 3\text{N}$ -Flag- $\delta$  were induced with tetracycline (1  $\mu\text{g}/\text{ml}$  final concentration, Life Technologies) and 5 mM sodium butyrate (Sigma-Aldrich, St. Louis, MO) for 24 hours and harvested in 10 ml per ten 15 cm-dishes of 10 mM HEPES, 1 mM EDTA (buffer A) freshly supplemented with protease inhibitors and 1 mM PMSF (final concentration) at 4°C with all subsequent purification procedures carried out at 4°C. Cells were homogenized with three cycles of 10 s each separated by 30 s intervals (Ultra Turrax T25, IKA Works, Wilmington, NC), followed by 20 strokes in Kontes-Duval glass tissue grinder. Homogenate was centrifuged at 43,000 x g for 30 min at 4°C and the pellet was resuspended in the buffer A and the entire procedure repeated. The resulting pellet was resuspended in the buffer A and a final homogenization carried out by aspiration with a 21-gauge needle and expelled through 27-gauge needle. Concentration of total protein was assessed with the Pierce BCA protein assay kit (Pierce, Rockford, IL). Under constant stirring, the membrane fraction was solubilized over 30 min by dropwise addition of 30 mM DDM (Anatrace, Maumee, OH) in buffer B (50 mM Tris/HCl, 150 mM NaCl, 2 mM CaCl<sub>2</sub>, 5 mM KCl, 5 mM MgCl<sub>2</sub>, 4 mM EDTA, pH 7.5) and 10% glycerol, supplemented with protease inhibitors and 1 mM PMSF, with the volume adjusted to produce an effective protein concentration of 1 mg/ml. Following an additional 2 hours of solubilization, the solution was centrifuged at 45,000 x g for 30 min at 4°C. Insoluble material in the pellet was discarded and the supernatant was stored in liquid nitrogen overnight.

After washing once with buffer B, 2 ml of Flag beads (Sigma-Aldrich) were pre-treated overnight at 4°C on polypropylene columns (Qiagen, Hilden, Germany) with 1.5 ml of 10 mg/ml poly-d-Lysine hydrobromide with gentle agitation. On the following day, beads were washed three times with six 2-ml volumes of buffer B with 10% glycerol and incubated with solubilized membrane fractions with gentle agitation for 2 hours. Once transferred back into propylene columns, beads were washed once with wash buffer (17 mM CHAPS, 8.5 mM asolectin in buffer B with 10% glycerol, homogenized with glass grinder and sonicated for 10 min), equilibrated with the same buffer for 1 hour with agitation and washed again. Two more washes with elution buffer (5 mM CHAPS, 200  $\mu\text{M}$  asolectin in buffer B with 10% glycerol, prepared as with wash buffer) were performed prior to elution of receptors by incubation with two x 2-ml of elution buffer supplemented with 0.15 mg/ml of Flag peptide (Sigma-Aldrich) for 2 hours with gentle rocking (elution 1). Second elution (elution 2) and another overnight incubation with 2-ml (elution 3) followed. Preparations with 200  $\mu\text{M}$  defined lipids (DOPC: DOPS:Cholesterol) instead of 200  $\mu\text{M}$  asolectin produced comparable results.

Different protease inhibitor cocktails and their concentrations were assessed with regards to  $\alpha 4$ -subunit fragmentation: 1. 1:100 dilution of Protease inhibitor cocktail (Sigma-Aldrich); 2. addition of 60 nM DAPT,  $\gamma$ -secretase inhibitor (Tocris, Minneapolis, MN); 3. blend of 10  $\mu\text{g}/\text{ml}$  Pepstatin A, 10  $\mu\text{g}/\text{ml}$  Leupeptin, 10  $\mu\text{g}/\text{ml}$  Chymostatin and 2  $\mu\text{g}/\text{ml}$  Aprotinin (all from Sigma-Aldrich); 4. Complete protease inhibitor cocktail tablets at suggested or doubled concentration (Roche, Indianapolis, IN); 5. supplementation with 1 mM PMSF at membrane preparation stage or continuously throughout the procedure to address the short half-life of

the compound. No reproducible and substantial differences were observed with regards to protease inhibitors used between individual preparations.

### Western blotting and deglycosylation

Purified protein was resolved on hand-casted 10% SDS-PAGE gels, loading approximately 10  $\mu$ g of protein (as determined by Pierce BCA assay, Thermo Scientific, Rockford, IL) with 4x Laemmli buffer (Bio-Rad, Hercules, CA) supplemented with 10%  $\beta$ -mercaptoethanol (Sigma). Following transfer onto PVDF membranes (Immobilon-FL, Millipore, Billerica, MA) in 20% MeOH transfer buffer, membranes were washed with MeOH, air dried, re-wetted and blocked with Odyssey blocking buffer (PBS, Li-Cor, Lincoln, NE) for 1 hour at room temperature. Membranes were incubated overnight with the antibodies indicated in the figure legends, diluted in blocking buffer supplemented with 0.2% Tween-20, at 4°C with gentle rocking. Following washes with 0.1% Tween-PBS, membranes were incubated with secondary antibodies in blocking buffer supplemented with 0.2% Tween-20 and 0.01% SDS, for 1 hour at room temperature. Blots were imaged on an Odyssey Classic Infrared Imager (Li-Cor), images were quantified using the Rectangle tool in Image Studio Lite v5.2.5 (Li-Cor), by encompassing signal from both channels in a single oblong shape. Images were converted to gray scale for each channel separately and contrast and brightness adjusted uniformly for readout convenience. All antibodies used, along with their dilutions, are listed in [S2 Table](#).

Deglycosylation of receptor subunits was carried out using PNGase F (NEB, Ipswich, MA) according to the manufacturer's guidelines, and protein was resolved using 10% NuPAGE Bis-Tris gel (Life Technologies, Carlsbad, CA) in NuPAGE running buffer (Life Technologies), according to the manufacturer's guidelines, with the remaining process as described before.

Coomassie Blue staining of the gels was performed on NuPAGE gels. Gels were fixed in 45% methanol, 10% acetic acid, 45% water (v/v/v), stained for 45 min in the same buffer supplemented with 0.125% Brilliant Blue R (Sigma) (w/v) and destained for 2–3 h using 40% methanol, 10% acetic acid and 50% water. Gels were dried and scanned.

### Electrophysiology

HEK 293 cells stably expressing tetracycline inducible  $\alpha 4\beta 3\delta$ -Flag or N-Flag- $\alpha 4\beta 3$  GABA<sub>A</sub> receptors were cultured on glass coverslips and induced with tetracycline (2  $\mu$ g/ml) 24 hours before recordings. The coverslips were placed in a recording chamber and perfused with the bath solution. Cells were voltage clamped at -50 mV using the patch clamp amplifier (Axopatch 200A, Molecular Devices, Sunnyvale, CA). GABA<sub>A</sub> receptor-mediated chloride currents from HEK cells were recorded using the whole-cell configuration of patch-clamp electrophysiology. Data was acquired using Clampex version 8.1 (Molecular Devices), digitized at 10 kHz and filtered at 5 kHz. Current traces were analyzed using Clampfit version 9 (Molecular Devices). Series resistance ranged from 0.5–4 M $\Omega$  and cell capacitances from 9–18 pF. Membrane-capacitance and series-resistance were compensated electronically by > 85% with a lag of 10  $\mu$  seconds. Drugs were delivered via a multichannel superfusion pipette coupled to a piezoelectric elements that switched superfusion solution in < 1 millisecond [17]. The recording chamber was continuously perfused with the bath solution in mM: 145 NaCl, 5 KCl, 10 HEPES, 2 CaCl<sub>2</sub>, and 1 MgCl<sub>2</sub>, 10 glucose, pH 7.4 (pH adjusted with N-methyl glucosamine). The pipette solution for whole-cell recordings contained in mM: 140 KCl, 10 HEPES, 1 EGTA and 2 MgCl<sub>2</sub> at pH 7.3 (pH adjusted with KOH). Open pipette resistances ranged from 1.6–3 M. Errors are standard deviation from at least three replicas.

## Statistical analysis

Statistical analysis for electrophysiology was done using GraphPad Prism 6. The GABA EC<sub>50</sub> was determined using Origin 6 software (OriginLab). Analysis of the [<sup>3</sup>H]muscimol binding was carried out using Igor Pro 7 (WaveMetrics). For Western blotting, the ratio of the signal intensity of individual antibodies for each sample was determined. Pooled (weighted) mean and standard deviation was determined for each receptor and p value determined by two-tailed unpaired Student's t-test, using GraphPad QuickCalcs software.

## Results and discussion

### Development of a stable, inducible HEK293-TetR $\alpha 4\beta 3\text{N-Flag-}\delta$ GABA<sub>A</sub>R cell line

The ratio of transfected cDNAs encoding individual GABA<sub>A</sub>R subunits can affect stoichiometry of  $\delta$ -subunit-containing pentamers, therefore affecting the EC<sub>50</sub> of the GABA concentration-response curve. In some cases, Hill coefficients of less than one have been reported, indicating heterogeneity [8, 10, 18].

We chose to transfect HEK293-TetR cells with constructs in the weight ratio of  $\alpha 4:\beta 3:\delta$  2:1:0.25, which was shown to produce stoichiometry of  $(\alpha 4)_2(\beta 3)_2(\delta)_1$  in a systematic study assessing this relationship by Western blotting of  $\alpha$ -bungarotoxin tagged subunits [11]. Our reasoning was further supported by the reported elevated stability of the  $\delta$ -subunit [10]. We placed a Flag-tag on the  $\delta$ -subunit so that affinity purification would yield only those expressed heteropentamers that contained  $\delta$ -subunits. The cell line expressing  $\alpha 4\beta 3$ , with Flag-tag on the N-terminal of  $\alpha 4$ -subunit, was constructed in analogous manner to serve as a control in the experiments.

HEK293 Tet-R cells transfected with aforementioned ratio of subunits underwent antibiotic selection and FACS sorting using a fluorophore-conjugated antibody against the Flag-tagged  $\delta$ -subunit. Individual cells were collected to establish monoclonal populations in a 96-well format (S1 Fig). Flow cytometry analysis allowed us to identify several candidate clones with high expression of the protein of interest, which were subsequently screened in a functional [<sup>3</sup>H]muscimol binding assay. The clone used in this study yielded  $19.1 \pm 3.1$  pmol of [<sup>3</sup>H]muscimol binding sites per mg of membrane protein (n = 17). This is comparable to that of the inducible  $\alpha 1\beta 3\gamma 2\text{L}$  cell line we previously reported [13].

The specific activity of receptors in cell membranes increased over 48 hours of induction time, reaching ~30 pmol/mg of total membrane protein. However, we routinely induced for 24–30 hours in order not to stress the cells. For the five inductions averaged in Table 1, the yield in the harvested cell membranes was  $75 \pm 9$  pmol/plate with a specific activity of  $17.2 \pm 2.8$  pmol [<sup>3</sup>H]muscimol binding sites/mg of membrane protein.

### Electrophysiological and pharmacological characterization of the $\alpha 4\beta 3\text{N-Flag-}\delta$ GABA<sub>A</sub>R cell line

We first characterized this GABA<sub>A</sub>R expressed in the plasma membrane 24–30 hours after induction. Because  $\alpha 4\beta 3\delta$  receptors expressed in oocytes often appear to have different gating kinetics such as low Hill coefficient and very low EC<sub>50s</sub> [7, 8], we will only compare the properties of our cell line's receptors, wherever possible to those in other mammalian expression systems.

DS2 is a specific positive allosteric modulator of  $\delta$ -subunit containing receptors [6], therefore, to confirm the incorporation of  $\delta$ -subunits in the GABA<sub>A</sub>R complex, we tested DS2 modulation of GABA<sub>A</sub>R mediated currents (Fig 1A). We employed a notch protocol herein,

**Table 1. Representative yield of  $\alpha 4\beta 3N$ -Flag- $\delta$  GABA<sub>A</sub>R purification by anti-Flag affinity chromatography.**

Purification fractions	Total specific [ <sup>3</sup> H]muscimol binding sites (pmol) <sup>a</sup>	% overall yield $\pm$ standard deviation <sup>b</sup>	Average [3H]muscimol specific activity <sup>b</sup>
Starting membranes	4577	100	17 $\pm$ 2.8 pmol / mg
Solubilized supernatant Applied on column	3927	80 $\pm$ 4.3	12 $\pm$ 1.5 pmol / ml
Flow through during binding	837	23 $\pm$ 3.0	3.6 $\pm$ 0.82 pmol / ml
First wash flow through	67	1.2 $\pm$ 0.21	2.1 $\pm$ 1.1 pmol / ml
Elution 1 (E1)	723	13 $\pm$ 1.4	54 $\pm$ 12 pmol / ml
E2	188	3.0 $\pm$ 1.3	24 $\pm$ 13 pmol / ml
E3	203	3.1 $\pm$ 1.0	26 $\pm$ 10 pmol / ml
Total elution	1114	20 $\pm$ 3	39 $\pm$ 12 pmol / ml

<sup>a</sup>Total amount of GABA<sub>A</sub>R, measured as specifically bound [<sup>3</sup>H]muscimol (250–500 nM) sites from one representative purification using 60 plates of cells.

<sup>b</sup> Mean  $\pm$  standard deviation of five purifications.

<https://doi.org/10.1371/journal.pone.0191583.t001>

characterized by short co-application of drug one second after GABA application (Fig 1A; middle column). In cells expressing  $\alpha 4\beta 3N$ -Flag- $\delta$  receptors, DS2 (10  $\mu$ M) enhanced maximum GABA elicited currents by 230  $\pm$  63% (SD, n = 6; Fig 1A, top panel); whereas, in cells expressing only N-Flag- $\alpha 4\beta 3$  receptors, DS2 produced only a mild enhancement of 12  $\pm$  7% (n = 6; differs from  $\alpha 4\beta 3N$ -Flag- $\delta$  with p = 0.0001; Fig 1A, bottom panel). Therefore, these data confirmed the incorporation of the  $\delta$ -subunit in the GABA<sub>A</sub>R complex in the  $\alpha 4\beta 3N$ -Flag- $\delta$  GABA<sub>A</sub>R cell line.

It is a characteristic of  $\alpha 4\beta 3\delta$  GABA<sub>A</sub>R that GABA acts as a partial agonist, opening only a fraction of the available channels (i.e. it has a low P<sub>open</sub>) [19, 20]. Using the above notch protocol, etomidate (10  $\mu$ M) enhanced the maximum GABA elicited currents by 540  $\pm$  235% (n = 7; Fig 1B, top panels) in cells expressing  $\alpha 4\beta 3\delta$  receptors. This experiment provides an estimate of the efficacy of GABA. Thus, if we assume that co-application of 10 mM GABA with 10  $\mu$ M etomidate opens 100% of available channels, then 10 mM GABA opened only 17  $\pm$  6% (n = 7) of available channels, indicating GABA is a low efficacy agonist of the  $\alpha 4\beta 3N$ -Flag- $\delta$  receptors, as has been previously reported for  $\alpha 4\beta 3\delta$  GABA<sub>A</sub>R [9, 20, 21]. In the control N-Flag- $\alpha 4\beta 3$  cell line, the etomidate enhancement was similar (490  $\pm$  84%, n = 4; Fig 1B, lower panel) suggesting that inclusion of the  $\delta$ -subunit does not change GABA's efficacy. On the other hand, introduction of the  $\delta$ -subunit into  $\alpha 4\beta 3$  receptors did dramatically increase the rate of current decay during the 4-s co-activation of GABA with etomidate (Fig 1B, middle panels).

The half-stimulatory GABA concentration (GABA EC<sub>50</sub>) was determined by normalizing peak current amplitudes obtained by the application of eight-second pulses of varying concentrations of GABA (0.1–100  $\mu$ M) to the peak amplitude value obtained with 10 mM GABA for the same cell (S2 Fig). The data was plotted against the GABA concentration and fitted with the Hill equation to yield a GABA EC<sub>50</sub> value of 2.1  $\pm$  0.28  $\mu$ M and a Hill coefficient of 1.5  $\pm$  0.24 (n = 3–5 cells at each point; Fig 2A), similar to previous values reported for  $\delta$ -containing receptors in mammalian cells [9, 22, 23].

The kinetics of the activation phase of currents were well fit by a single exponential whose time constant,  $\tau$ , decreased with increasing GABA concentration, from 165  $\pm$  20 ms at 0.1  $\mu$ M GABA (n = 3) to 6  $\pm$  1 ms at 100  $\mu$ M GABA (n = 3), above which (0.3–10 mM) there was no increase, probably because of our limited solution exchange rate of 2–5 ms. The initial rate was linear up to  $\sim$ 10  $\mu$ M and could be fit to the rate equation

$$k_{Act} = k_{-1} + (k_{+1} \times [GABA]),$$

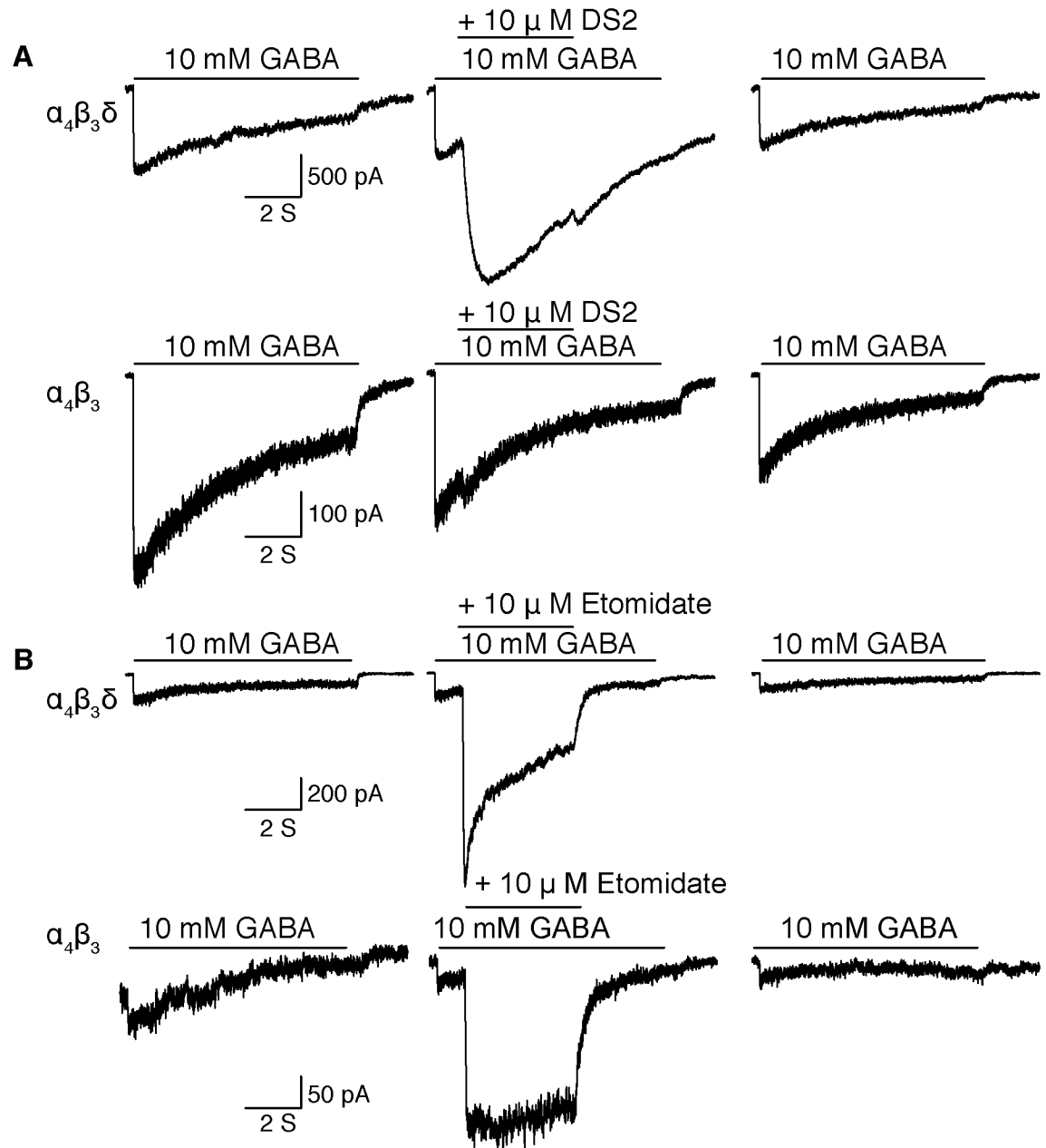


**Fig 1. The  $\delta$ -subunit is expressed in the  $\alpha 4\beta 3N$ -Flag- $\delta$  GABA<sub>A</sub>R stable cell line.** Representative current traces show the effect of DS2 (A) and Etomidate (B) on 10 mM GABA-elicited currents on  $\alpha 4\beta 3N$ -Flag- $\delta$  (upper panel) compared to N-Flag- $\alpha 4\beta 3$  (lower panel). Currents were elicited in a notch protocol by an eight second pulse of GABA, during which drug was co-applied for 4 seconds 1 second after the GABA perfusion started. Concentrations are indicated in the figure.

<https://doi.org/10.1371/journal.pone.0191583.g001>

where  $k_{Act}$  is the measured activation rate following addition of GABA ( $1/\tau$ ), and  $k_{+1}$  and  $k_{-1}$  are the apparent forward and reverse GABA binding rates. A plot of these data yielded  $k_{+1} = 5.7 \pm 0.2 \times 10^6 \text{ s}^{-1}\text{M}^{-1}$  and  $k_{-1} = 5 \pm 1 \text{ s}^{-1}$ , yielding an apparent dissociation constant of  $0.9 \pm 0.2 \mu\text{M}$ . In  $\alpha 4\beta 3\gamma 2$  receptors on the other hand,  $k_{+1}$  was  $6 \times 10^6 \text{ s}^{-1}\text{M}^{-1}$ , a value similar to our value for  $\alpha 4\beta 3\delta$  receptors, but  $k_{-1}$  was 20-fold faster ( $100 \text{ s}^{-1}$ ) than in  $\alpha 4\beta 2\delta$  receptors [21].



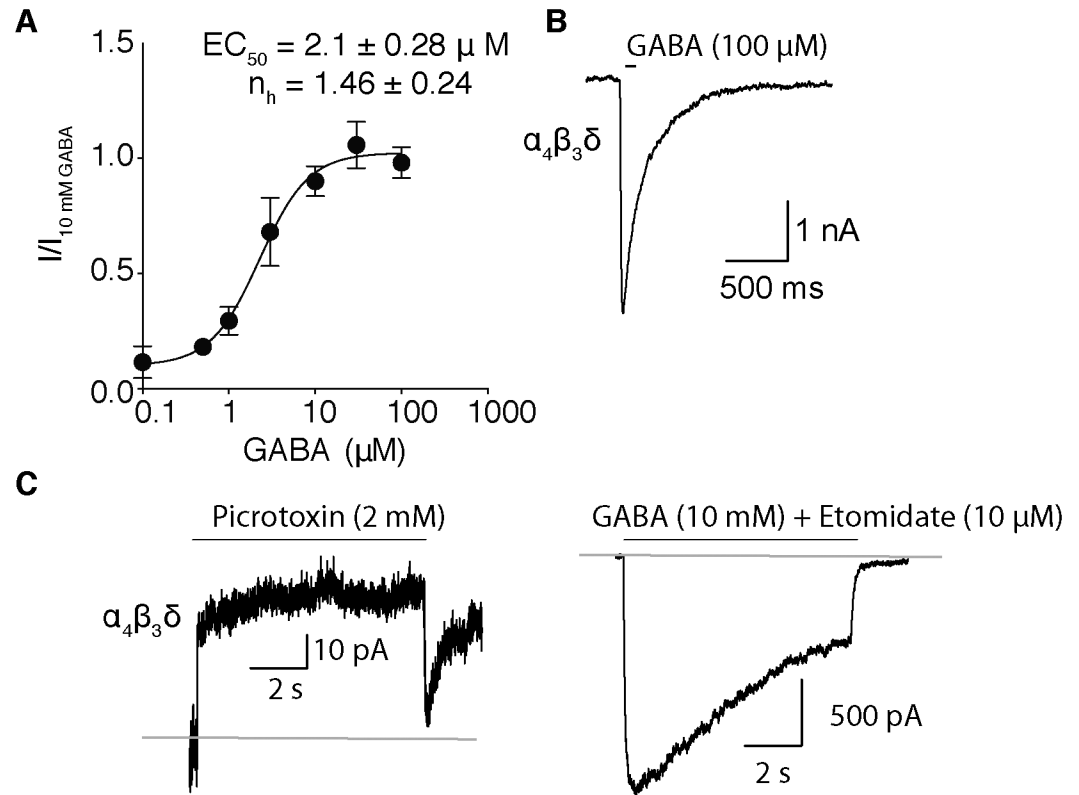


**Fig 2. The gating properties of  $\alpha 4\beta 3\delta$  GABA<sub>A</sub>Rs.** (A) GABA concentration-response curve for  $\alpha 4\beta 3\delta$  receptor mediated currents. Currents were elicited by application of varying concentrations of GABA (0.1–10 mM). Peak current amplitudes in each cell were normalized to that obtained with 10 mM GABA. (B) Representative current trace obtained by application of an 8.5 ms pulse of 100  $\mu$ M GABA to measure the deactivation rate. (C)  $\alpha 4\beta 3\delta$  receptors are spontaneously open. (Left panel) Representative trace of outward currents observed by application of 2 mM PicROTOXIN to inhibit the spontaneously open receptors. (Right panel) The estimate of the maximum inward currents obtained by co-application of 10 mM GABA with 10  $\mu$ M Etomidate to gate all available receptors. The gray lines are drawn by eye to represent the baseline. At least three cells per concentration were used throughout experiments.

<https://doi.org/10.1371/journal.pone.0191583.g002>

This accounts for the 20-fold higher apparent dissociation constant and GABA EC<sub>50</sub> characteristic of GABA<sub>A</sub>Rs with a  $\gamma$ -subunit.

In a recent study of  $\alpha 1\beta 3\delta$  GABA<sub>A</sub>Rs in HEK cell lines, Botzolakis, *et al.* [10] reported 10–90% rise times at 1 mM GABA ranging from 4–22 ms depending on the construct ratio. We note however that all these rise times are considerably faster than ~100 ms at 100  $\mu$ M GABA previously reported by Brown *et al* in  $\alpha 4\beta 3\delta$  receptors [22]. Although their solution exchange times were comparatively slow, 20–30 ms, the discrepancy might also be caused by the way the cell lines were constructed, which leaves uncertainties about the stoichiometry [22].

The rate of deactivation (channel closing) was measured after an 8.5 ms pulse of 100  $\mu$ M GABA, a time chosen to maximize current and minimize the contribution of desensitization before GABA is withdrawn (Fig 2B). At 100  $\mu$ M GABA, the closing phase of the current was best fit with two exponentials that had time constants of  $1100 \pm 440$  and  $175 \pm 50$  ms (6 cells). The fastest phase occupied  $76 \pm 12\%$  of the total current decay amplitude. The deactivation kinetics were independent of GABA concentration because similar values were obtained at 10 mM GABA. Our values may be compared to that of ~400 ms reported by Brown *et al* in  $\alpha 4\beta 3\delta$  receptors using a lower time resolution perfusion system [22]. In another study of  $\alpha 1\beta 3\delta$  receptors, the deactivation rate varied somewhat with the ratio of constructs used in the

transfection from 100–200 ms; at a ratio of 1:1:0.3, the closest condition to ours, their value was ~170 ms, not different from our faster value [10]. Using the concatenated subunits  $\beta 3-\alpha 1-\delta/\beta 3-\alpha 1$ , Liu et al. found a deactivation time constant of ~50 ms [24].

The high density of GABA<sub>A</sub>Rs that can be achieved in our inducible cell line yields larger currents that allow spontaneous activity to be clearly observed. Thus, application of 2 mM picrotoxin, a specific blocker of GABA<sub>A</sub> receptors, for 8 seconds revealed an outward current, suggesting that spontaneously open receptors were being inhibited (Fig 2C). The fraction of spontaneously open receptors was estimated to be about  $3.2 \pm 0.6\%$ , by assuming that the outward current activated by an 8-s pulse of GABA (10 mM) co-applied with etomidate (10  $\mu$ M) opened all the receptors expressed in the same cells after washout of PTX (Fig 2C, right panel). This small amount of spontaneous activity is consistent with a single channel study in which HEK cells were transiently transfected with rat or human  $\alpha 4:\beta 3:\delta$  cDNAs in the ratio 1:1:1 [25].

The desensitizing phase of the currents during an 8-sec exposure to GABA (1–100  $\mu$ M) was best fit by a single exponential and did not vary significantly with GABA concentration. A desensitization time constant,  $\tau$ , of  $2.6 \pm 0.9$  s was obtained when times from all GABA concentrations were averaged. Brown et al reported a  $\tau$  of 4.8 s at 100  $\mu$ M GABA in their  $\alpha 4\beta 3\delta$  cell line [22]. The degree of desensitization was different from that reported by Botzolakis et al. for  $\alpha 1\beta 3\delta$  receptors [10]. Whereas in our  $\delta$  cell line we observed ~70% desensitization in 4 seconds at 100  $\mu$ M GABA, the latter workers observed little desensitization in 4 seconds at transfection ratios similar to ours, but 40–70% at much lower transfection ratios. In the concatenated subunits  $\beta 3-\alpha 1-\delta/\beta 3-\alpha 1$ , desensitization after 4 s at 1 mM GABA was ~40% with a time constant of 4.7 s [24].

### Solubilization, purification and reconstitution of the $\alpha 4\beta 3\delta$ GABA<sub>A</sub>Rs into CHAPS/lipid micelles

Receptors were purified following the procedure of Dostalova et al. with minor modifications discussed below [12, 13]. An SDS-PAGE gel loaded with samples from each stage of the procedure illustrates the progress of the purification (S3 Fig). In one purification (Table 1, column 2), membrane fractions extracted from cells grown on sixty 15-cm plates containing 4.6 nmol of [<sup>3</sup>H]muscimol binding sites yielded 1.1 nmol of purified receptor. In the average of five purifications (Table 1, columns 3 & 4), 20% of binding sites were lost during membrane solubilization with 30 mM DDM and a further 23% was not retained on anti-Flag affinity chromatography beads. After washing, purified receptors were equilibrated in 5 mM CHAPS and 200  $\mu$ M lipid. The nature of the lipid had no major influence on the purified receptor's properties. The lipids used were asolectin, DOPC:DOPA:cholesterol or DOPC:DOPS:cholesterol in the molar ratio 52:15:33. Following three consecutive elutions with 0.15 mM Flag peptide, the combined average yield of receptor was 20%, corresponding to  $0.9 \pm 0.2$  nmol per ml of [<sup>3</sup>H]muscimol binding sites from 60 plates with specific activity of  $39 \pm 12$  pmol per ml of combined eluted fractions.

### Characterization of $\alpha 4\beta 3\delta$ -Flag- $\delta$ GABA<sub>A</sub>R by radioactive ligand binding assays

Binding of the GABA<sub>A</sub>R agonist [<sup>3</sup>H]muscimol to cell membranes was displaceable by GABA. The displaceable binding increased with [<sup>3</sup>H]muscimol concentration reaching a plateau at about 100 nM (Fig 3). The data were fitted by nonlinear least squares to the Hill equation, yielding an EC<sub>50</sub> of  $9.2 \pm 0.6$  nM, a Hill coefficient of  $1.1 \pm 0.03$  and  $22.6 \pm 0.5$  pmol of sites per mg of membrane protein. This apparent affinity is respectively equal to and 5-fold higher than

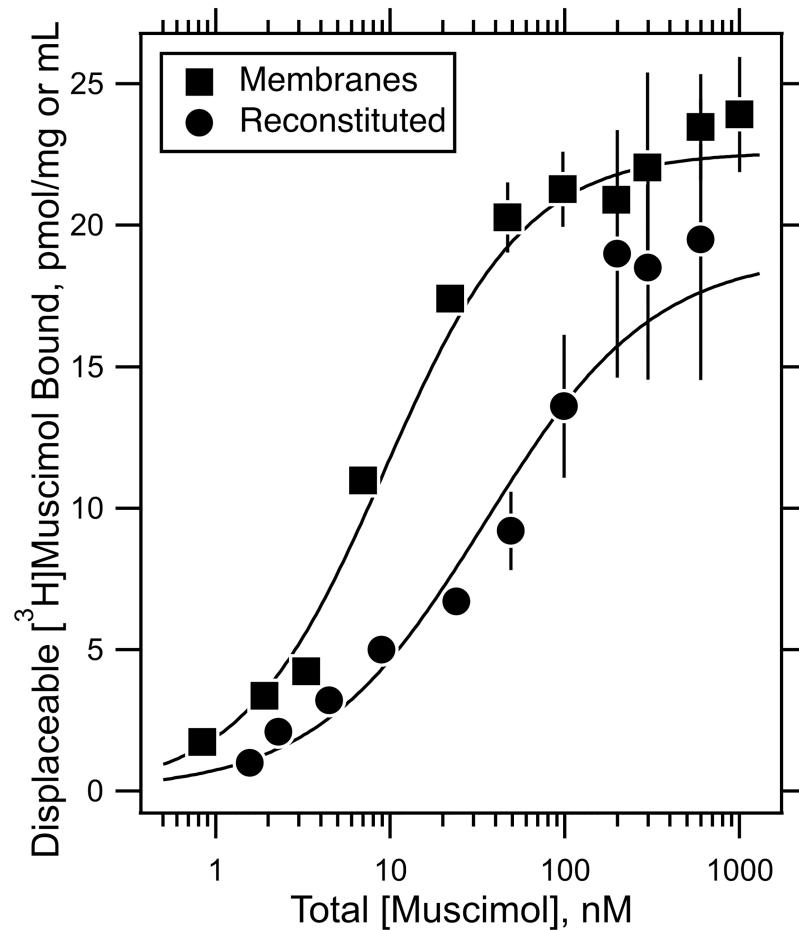


**Fig 3. The binding isotherm of the agonist  $[^3\text{H}]$ muscimol to the  $\alpha 4\beta 3\text{N}$ -Flag- $\delta$  GABA<sub>A</sub> receptor in native membranes and reconstituted into CHAPS/lipid micelles.** Binding curves of  $[^3\text{H}]$ muscimol to  $\alpha 4\beta 3\text{N}$ -Flag- $\delta$  GABA<sub>A</sub>Rs, both, in cell membranes (pmol/mg membrane protein) and after purification and reconstitution into micelles of 5 mM CHAPS and 200  $\mu\text{M}$  DOPC:DOPS:Cholesterol in mole ratio 52:15:33 (pmol/mL). Displaceable binding was determined as the difference between binding in the presence and absence of 1 mM GABA using a filtration assay in triplicate. The displaceable binding and its standard deviation was determined by subtracting these two values and propagating errors at each total muscimol concentration. The curves were fitted by nonlinear least squares with weighting by standard deviation. These yielded apparent dissociation constants of  $9.2 \pm 0.6$  and  $35 \pm 12$  nM, respectively. The  $B_{\text{max}}$  of the membranes was  $22.6 \pm 0.5$  pmol/mg and for reconstituted receptors in micelles was  $19 \pm 3$  pmol/mL. The Hill coefficients differed little from one ( $1.07 \pm 0.3$  and  $0.90 \pm 0.05$  respectively).

<https://doi.org/10.1371/journal.pone.0191583.g003>

in our previously developed  $\alpha 1\beta 3$  and  $\alpha 1\beta 3\gamma 2$  GABA<sub>A</sub>R cell lines [13, 26]. A similar 5-fold differential has been noted previously in a study in which GABA<sub>A</sub>Rs containing either  $\gamma$ - or  $\delta$ -subunits were selectively immuno-precipitated from rat brain, although the absolute values were smaller than ours [27].

After receptors were reconstituted into CHAPS/DOPC:DOPS:Cholesterol micelles they exhibited a higher apparent dissociation constant of  $35 \pm 12$  nM compared to membranes (Fig 3). A preliminary value in CHAPS/asolectin also yielded a higher value compared to membranes [28]. Such a difference between membranes and micellar receptors has been noted before [13], and we suspect it comes from a modulatory action of CHAPS that favors a lower affinity conformation.

The  $\delta$ -subunit specific agent DS2 at 30  $\mu\text{M}$  enhanced displaceable  $[^3\text{H}]$ muscimol (2 nM) binding by  $142 \pm 12\%$  ( $n = 10$ ) in membranes and  $128 \pm 11\%$  ( $n = 7$ ) in GABA<sub>A</sub>Rs

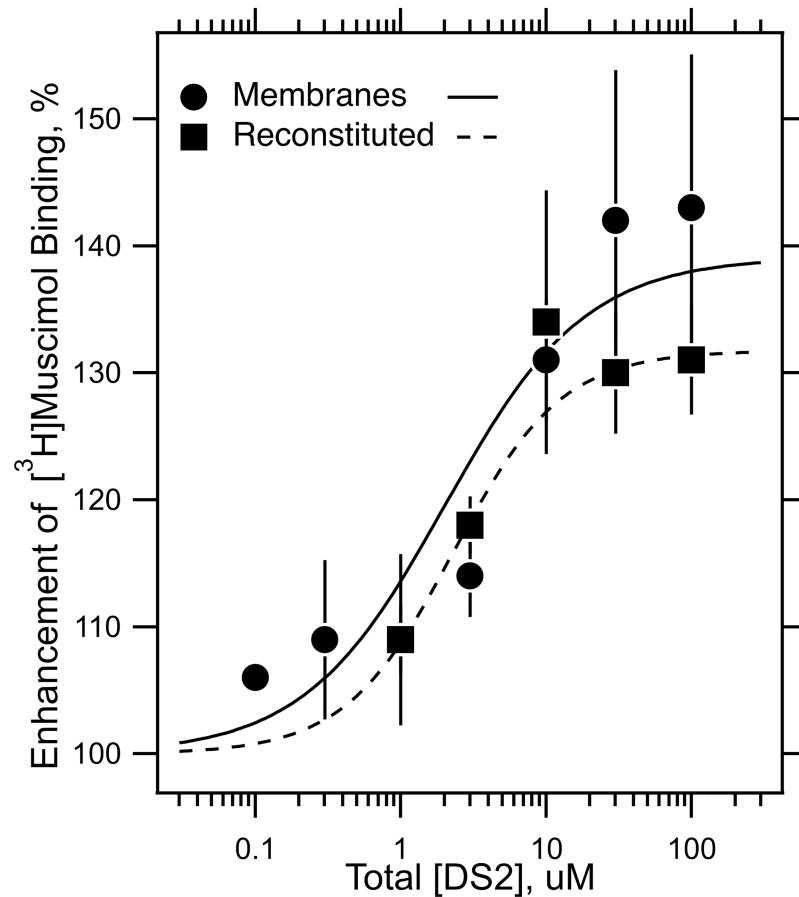


**Fig 4. DS2 enhances agonist binding in  $\delta$ -subunit containing receptors.** The  $\delta$ -subunit specific modulator, DS2, modulates [<sup>3</sup>H]muscimol binding (2 nM) in  $\alpha 4\beta 3\text{N}$ -Flag- $\delta$  GABA<sub>A</sub>Rs. For the membranes, the data are the mean and standard deviation of two experiments, and for micelle reconstituted receptors for a single experiment in triplicate. The curves were fitted by nonlinear least squares to the Hill equation. The EC<sub>50</sub> (μM), Hill coefficient and maximum modulation were: for membranes, 2.0 ± 0.7 μM, 0.9 ± 0.2, 139 ± 4%; for reconstituted 2.3 ± 0.8 μM, 1.2 ± 0.5, 132 ± 4%.

<https://doi.org/10.1371/journal.pone.0191583.g004>

reconstituted into CHAPS/lipid micelles (Fig 4). In a parallel reconstitution on the same day into CHAPS/asolectin or CHAPS/DOPC:DOPS:cholesterol, no difference in degree of enhancement was found. The concentration–dependence of DS2 modulation of 2 nM [<sup>3</sup>H] muscimol binding yielded an EC<sub>50</sub>s of 2.0 ± 0.7 μM for receptors in native membranes and 2.3 ± 0.8 μM for receptors reconstituted into CHAPS/PC:PS:Cholesterol micelles (Fig 4).

### Biochemical characterization of the CHAPS/asolectin reconstituted $\alpha 4\beta 3\text{N}$ -Flag- $\delta$ GABA<sub>A</sub> receptor

**All subunits are glycosylated.** Analysis of the purified and reconstituted  $\alpha 4\beta 3\text{N}$ -Flag- $\delta$  receptor into CHAPS/asolectin micelles by the means of SDS-PAGE followed by Western blotting indicated the presence of all three subunits as expected, however the observed molecular weight of each subunit was larger than predicted by the mature amino acid sequence. The  $\alpha 4$ -subunit presented at 72 and 54kDa (expected at 66kDa), the  $\beta 3$ -subunit presented as double band pattern of approximately 62 and 58kDa (predicted at 52kDa) and the  $\delta$ -subunit appeared as a ladder of three bands around 58kDa (predicted at 49kDa). This shift in mobility can be associated with post-translational modification in the form of an N-linked glycosylation

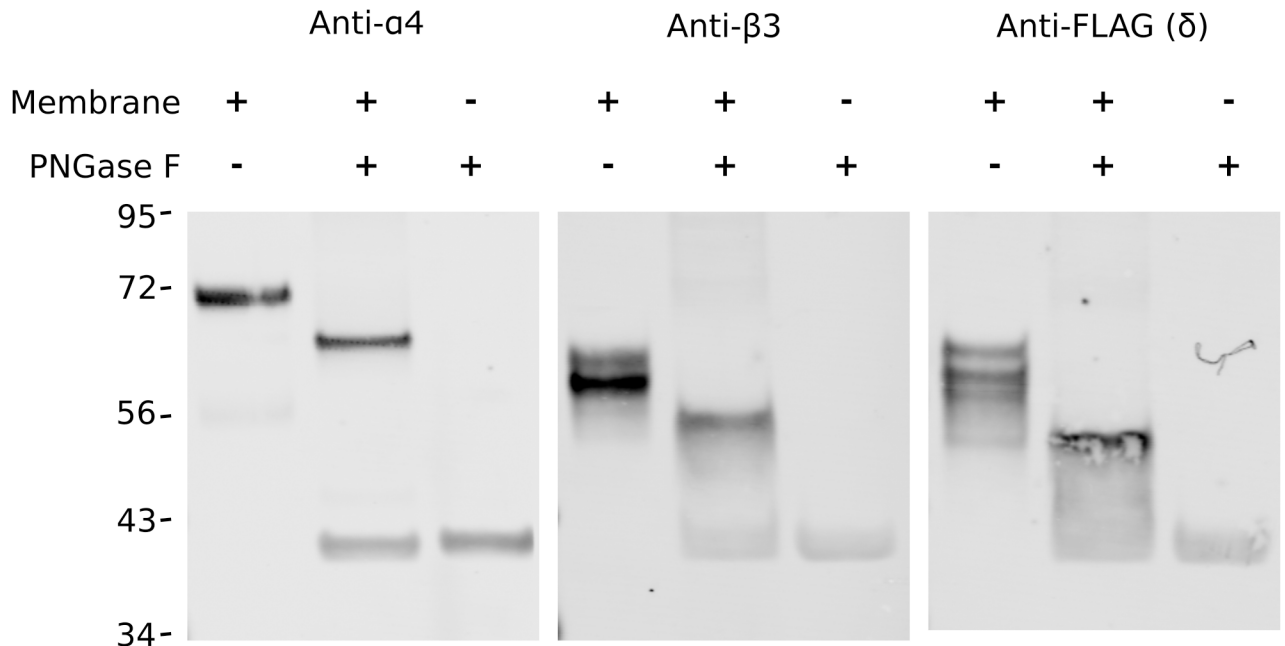


**Fig 5. All subunits of the  $\alpha 4\beta 3$ N-Flag- $\delta$  GABA<sub>A</sub> receptor are glycosylated.** Purified receptors were resolved by Western blotting with antibodies for  $\alpha 4$ - and  $\beta 3$ -subunits or Flag, as shown on the left, middle and right panels, respectively. In each of the three panels, reading left to right the lanes are: purified receptor; purified receptor after deglycosylation with PNGase F, and PNGase F alone. The band below the 43 kDa marker was nonspecific and associated with PNGase F. Numbers on the left side indicate MW in kDa. The  $\alpha 4$  and  $\beta 3$  antibodies are polyclonal. Brightness and contrast were uniformly adjusted for each panel.

<https://doi.org/10.1371/journal.pone.0191583.g005>

commonly described for the GABA receptors [29]. Indeed, after *in vitro* deglycosylation of the purified receptors by the relatively nonspecific PNGase F (Fig 5), the molecular weight of each subunit decreased by approximately 5–10 kDa.

**Origin of  $\alpha 4$  fragmentation.** The appearance of two bands upon immunoblotting for  $\alpha 4$  has been reported previously [30]. We have reported previously that the identity of these bands was confirmed by the LC/MS/MS [28]. Furthermore, Western blotting of the CHAPS/asolectin reconstituted N-Flag- $\alpha 4\beta 3$  receptor with anti-Flag and anti- $\alpha 4$  antibodies produced matching bands (Fig 6A and S4 Fig). The extent of  $\alpha 4$  protein fragmentation, measured as a ratio of lower to higher molecular weight bands, varied greatly between independent protein preparations from 2% to 125% (n = 6). When cells were lysed with 4xLaemmli buffer upon suspension or directly in the well, no fragmented protein was observed (lanes 1 and 3), unless plasma membrane was previously disrupted by sonication or 10 mM DDM treatment (lanes 2 and 4; Fig 6B and S5 Fig). Fragmentation could be observed already during the preparation of the plasma membrane fraction and sometimes occurred during the micellar reconstitution process (Fig 6C and S6 Fig). This observation implies that the  $\alpha 4$ -subunit is synthesized intact and that fragmentation occurs during processing. However, we observed no correlation between protein fragmentation and the concentration or spectrum of protease inhibitors used throughout the purification process. Furthermore, incubation of the plasma membrane fraction at temperatures ranging from 4 to 37°C for 1 hour did not have any effect on protein fragmentation, suggesting that it is not an effect of enzymatic activity (Fig 6D and S7 Fig). Our previous work on  $\alpha 1\beta 3$  and  $\alpha 1\beta 3\gamma 2$  receptors utilized the same purification procedure without any fragmentation of the  $\alpha 1$ -subunit, suggesting that the large cytoplasmic loop of the  $\alpha 4$ -subunit is the problem (70 residues in  $\alpha 1$  subunit vs. 161 in  $\alpha 4$ ). While this is unfortunate, it is quite possible that the pentamer remains intact. For example, crystallization of the homopentameric serotonin

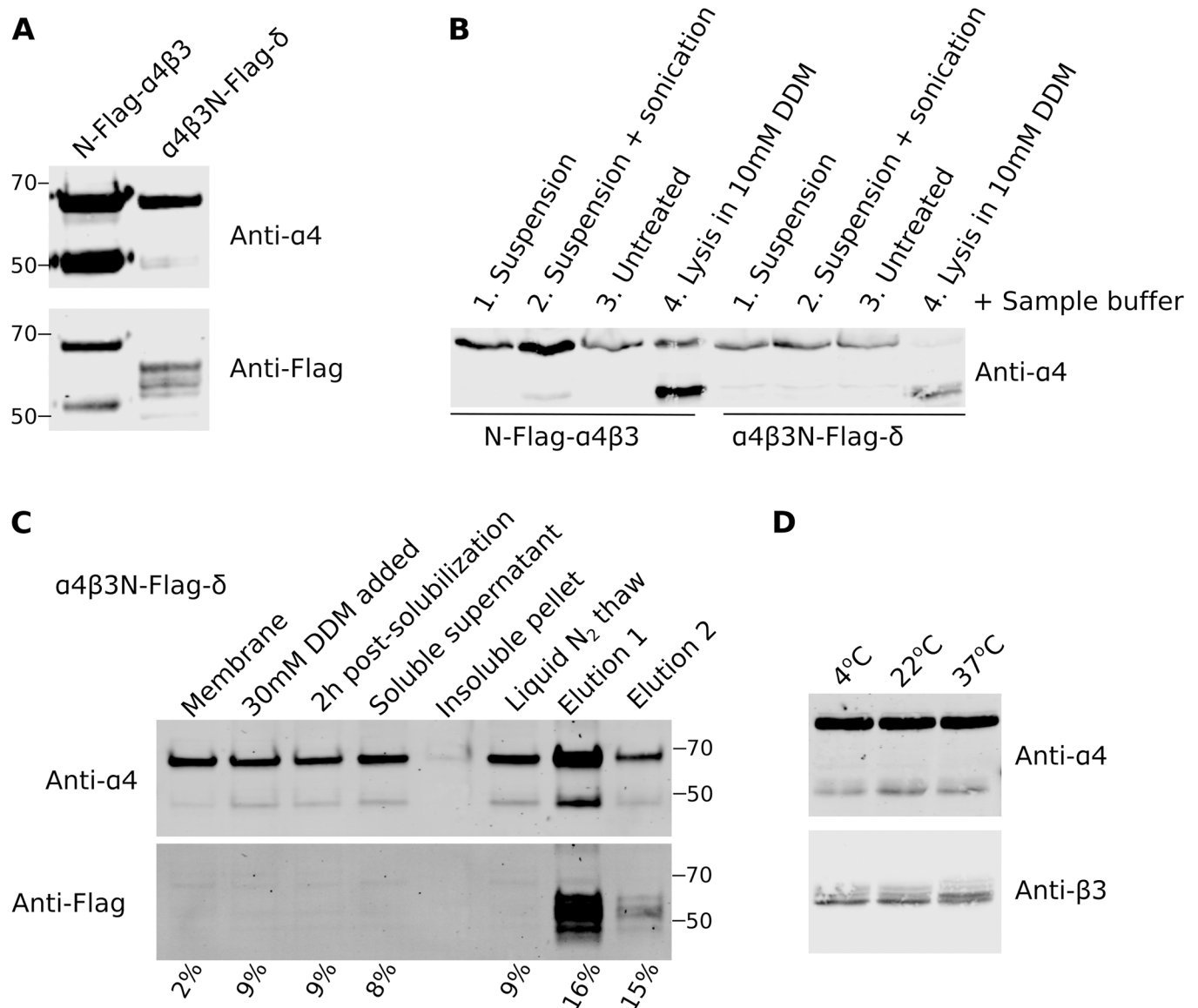


**Fig 6. Stability of the  $\alpha 4$ -subunit.** (A) Western blot depicting fragmentation of  $\alpha 4$ -subunit seen as two bands in N-Flag- $\alpha 4\beta 3$  and  $\alpha 4\beta 3$ N-Flag- $\delta$  receptors reconstituted into CHAPS/asolectin micelles is presented. Both  $\alpha 4$  bands are identified by polyclonal anti- $\alpha 4$  and monoclonal anti-Flag antibodies in the former receptor, confirming identity of the band. Numbers on the side indicate the position of the molecular weight markers (kDa). (B) Cells induced to express indicated GABA<sub>A</sub>Rs were prepared for Western blotting by either 1. suspending cells in suspension buffer; 2. suspending and sonicating; 3. leaving in a monolayer (untreated); or 4. lysing directly in the well with suspension buffer supplemented with 10 mM DDM; as indicated, prior to lysing cells with a 4x Laemmli sample buffer with 10%  $\beta$ -mercaptoethanol. Suspension buffer was supplemented with Protease Inhibitor Cocktail (Sigma) at 1:100 dilution. (C) Representative Western blot of samples obtained during  $\alpha 4\beta 3$ N-Flag- $\delta$  receptor purification, as described in the materials and methods section. Numbers under each lane indicate the fraction the lower band comprises of the higher band, expressed as percentile points. (D) Membrane fraction from the  $\alpha 4\beta 3$ N-Flag- $\delta$  was incubated for 1 hour at indicated temperatures prior to analysis by Western blotting. All blots are presented as grayscale and were uniformly adjusted for brightness and contrast to facilitate analysis. Full immunoblots used to make panels A-D are presented as S4–S7 Figs.

<https://doi.org/10.1371/journal.pone.0191583.g006>

5-HT<sub>3A</sub> receptor was aided by cleavage in the extracellular domain, yet the C-terminal trans-membrane domain helix M4 remained part of the structure [31].

### Estimating the stoichiometry of $\alpha 4\beta 3$ N-Flag- $\delta$ GABA<sub>A</sub>Rs

The exact subunit stoichiometry of GABA<sub>A</sub>R pentamers containing the  $\delta$ -subunit remains uncertain, and indeed during development of this cell line it became more likely that several

stoichiometries may be possible [10]. Although our receptor was not optimally designed for stoichiometry determinations, we attempted to place some limits by utilizing the duplex capabilities of the near-infrared fluorescence detection system and comparing the ratio of two antibodies both in the N-Flag- $\alpha 4\beta 3$  receptor and in the  $\alpha 4\beta 3$ N-Flag- $\delta$  receptor after purification. As polyclonal anti- $\alpha 4$  and monoclonal anti-Flag antibodies recognize the same subunit in the former receptor, the observed signal ratio can be normalized to 1, allowing the molar ratio of  $\alpha 4$  to  $\delta$  to be determined in the latter receptor (S8 Fig). The  $\alpha 4$ :Flag( $\delta$ ) ratio for N-Flag- $\delta$  containing receptors was below 1 ( $0.40 \pm 0.28$  SD,  $n = 5$ ) compared to 1 ( $\pm 0.11$  SD,  $n = 5$ ) in N-Flag- $\alpha 4\beta 3$ , with  $p = 0.0073$  (two-tailed unpaired Student's *t*-test). However, because of the amount of processing required before quantifying the blots, there are likely to be systematic errors that are not included in the above statistics. Nonetheless, it is safe to conclude that there are not two  $\alpha$ -subunits for each  $\delta$ -subunit. This is consistent with the evidence that etomidate photolabels a site in the transmembrane domain between two  $\beta$  subunits in receptors from this same cell line [28].

Further characterization was less secure, requiring the comparison of the  $\alpha 4\beta 3$ N-Flag- $\delta$  and the N-Flag- $\alpha 4\beta 3$  receptors using a  $\beta 3$  monoclonal and an  $\alpha 4$  polyclonal antibody. We found that the ratio of  $\beta 3$ :  $\alpha 4$  in  $\alpha 4\beta 3$ N-Flag- $\delta$  was 1.68 ( $\pm 0.15$  SD,  $n = 4$ ) times higher than in N-Flag- $\alpha 4\beta 3$  (S9 Fig). If we assume a stoichiometry ( $\alpha 4$ )<sub>2</sub>( $\beta 3$ )<sub>3</sub> [11], then the measured ratio of  $\beta 3$ :  $\alpha 4$  in the  $\alpha 4\beta 3$ N-Flag- $\delta$  receptor is 2.5 ( $1.68 \times 3/2$ ), which is not inconsistent with the results in the preceding paragraph and suggests a possible stoichiometry of ( $\alpha 4$ )<sub>1</sub>( $\beta 3$ )<sub>3</sub>( $\delta$ )<sub>1</sub>. Other assumptions lead to different answers, so this assignment is not definitive. Nor can we rule out that there might be more than one pentamer stoichiometry present, although our functional titrations offer no hint (Figs 2 & 3). Indeed, the concept of variable stoichiometries has been suggested by several groups [10, 11, 32, 33], and was clearly observed by Wagoner and Czajkowski [11]. We conclude that structural studies will be required to resolve the stoichiometry.

## Conclusion

We have established an inducible cell line that yields  $\alpha 4\beta 3\delta$  GABA<sub>A</sub> receptors at high levels suitable for biophysical and biochemical studies. Our characterization shows the receptors in this cell line to have the gating and pharmacological properties to be expected of a GABA<sub>A</sub>R of this subunit composition. We performed a relatively detailed analysis of gating in order that these properties may be linked to structural studies that this cell line may eventually promote.

We have demonstrated that this receptor can be purified in CHAPS/lipid micelles while maintaining equilibrium allosteric interactions between the agonist and anesthetic binding sites in large enough quantities to enable studies of structure, dynamics and function. Such studies may definitively resolve many of the uncertainties that cannot be resolved by electrophysiological techniques alone. The strategy of using the Tet-R inducible cell line, which was introduced by the Khorana laboratory to study rhodopsin [16], to study large heteropentameric ligand-gated ion channels [12, 13] has already yielded a crystal structure of the 5HT<sub>3</sub> receptor and a dynamics study of a GABA<sub>A</sub>R in the vicinity of the etomidate-binding site [31, 34].

## Supporting information

**S1 Fig. Stages of establishing monoclonal HEK293 TET-R  $\alpha 4\beta 3$ N-Flag- $\delta$  stable cell line.** Panels A-D depict flow cytometry results at indicated stages of cell line development. (A) Transfected cells following antibiotic selection. (B) Cells as in panel A following 24 hours of tetracycline induction. (C) Monoclonal population of cells with the highest expression of

N-Flag- $\delta$  used in the study, confirmed to have approximately 19 pmol/mg [<sup>3</sup>H]muscimol binding sites in the membrane fraction. (D) Histogram of cells in panel C.

(TIF)

**S2 Fig. Representative normalized currents elicited by varying concentrations of GABA on  $\alpha 4\beta 3$ N-Flag- $\delta$  expressing cells.** Currents were recorded using whole cell patch clamp technique from cells exposed to 0.1; 0.5; 1; 3; 10; 30; 100  $\mu$ M of GABA for 8 seconds. Each concentration was recorded on 3–5 cells and peak amplitude was normalized to the recording obtained with 10 mM GABA on the same cell. Representative current for a single cell is shown.

(TIF)

**S3 Fig. Coomassie Blue staining of the SDS-PAGE.** Samples collected throughout the purification procedure were resolved on 10% SDS-PAGE gel under denaturing conditions. Second lane (membrane) was loaded with 30  $\mu$ g (0.86 pmol) of total membrane protein. Gel was subsequently fixed and stained with Coomassie Blue. A similar pattern was observed by Chiara and colleagues in photolabelling studies (Chiara *et al.*, 2016). The main bands observed in the elution fractions represent individual subunits of the  $\alpha 4\beta 3\delta$  GABA<sub>A</sub> receptor. Numbers to the right represent molecular weights of the markers. Number of pmols in the Elution fractions loaded was determined by [<sup>3</sup>H]muscimol binding assay. Contrast and brightness of the bottom panel were adjusted uniformly to facilitate inspection.

(TIF)

**S4 Fig. The  $\alpha 4$ -subunit is fragmented.** Whole immunoblot used to produce Fig 6A is presented. Two independent preparations for each reconstituted receptor is presented and those additional preparations flank the lanes shown in Fig 6A. Molecular weight standards are shown on the left hand side including their size in kDa. Lower two panels are greyscale representation of individual channels corresponding to immunoblot with antibodies as indicated.

(TIF)

**S5 Fig. The protein preparation procedure affect  $\alpha 4$ -subunit fragmentation.** Whole immunoblot used to produce Fig 6B is presented. Immunoblot with polyclonal anti- $\alpha 4$ -subunit antibody produced additional band above 70 kDa. This band was not observed on other occasions and it did not correlate with anti-Flag immunoblot on samples positive for N-Flag- $\alpha 4\beta 3$ , suggesting it to be non-specific.

(TIF)

**S6 Fig. Fragmentation of  $\alpha 4$ -subunit throughout the standard purification procedure.**

Whole immunoblot of  $\alpha 4\beta 3$ N-Flag- $\delta$  receptor used to produce Fig 6C is presented. Molecular weight markers are flanking with their respective size in kDa indicated on the left hand side.

(TIF)

**S7 Fig. Incubation of protein lysate at different temperatures does not affect  $\alpha 4$ -subunit fragmentation.** Whole immunoblot used to produce Fig 6D is presented. The molecular weight marker is shown on the left, with respective size indicated on the right hand side. The marker migrated at a slight angle.

(TIF)

**S8 Fig. Representative anti- $\alpha 4$  and anti-Flag duplex Western blot.** Reconstituted N-Flag- $\alpha 4\beta 3$  and  $\alpha 4\beta 3$ N-Flag- $\delta$  receptors from two independent purifications of each were analyzed by Western blotting. The bottom (color) panel represents the original membrane scan that was used for quantification. Grayscale panels are depicted to facilitate analysis. Immunoblots were



uniformly adjusted for brightness and contrast.  
(TIF)

**S9 Fig. Representative anti- $\alpha 4$  and anti- $\beta 3$  duplex Western blot.** Elution 1 and elution 2 fractions of the reconstituted N-Flag- $\alpha 4\beta 3$  and  $\alpha 4\beta 3$ N-Flag- $\delta$  receptors were analyzed by Western blotting. The bottom (color) panel represents the original membrane scan that was used for quantification. Grayscale panels are depicted to facilitate analysis. Immunoblots were uniformly adjusted for brightness and contrast.  
(TIF)

**S1 Table. Primers used in the study.**  
(DOCX)

**S2 Table. Antibodies used in the study.**  
(DOCX)

**S1 Text. Subunit amino acid sequences used in this study.**  
(DOCX)

## Acknowledgments

This work was supported by National Institutes of Health Grant GM-58448 and by the Department of Anesthesia, Critical Care & Pain Medicine, Massachusetts General Hospital. The content is solely the responsibility of the authors and does not necessarily represent the official views of the National Institutes of Health.

## Author Contributions

**Conceptualization:** Keith W. Miller.

**Formal analysis:** Rooma Desai, Wojciech J. Stec, Keith W. Miller.

**Funding acquisition:** Keith W. Miller.

**Investigation:** Xiaojuan Zhou, Rooma Desai, Yinghui Zhang, Wojciech J. Stec, Youssef Jounaidi.

**Methodology:** Xiaojuan Zhou, Rooma Desai, Yinghui Zhang, Wojciech J. Stec, Youssef Jounaidi.

**Project administration:** Keith W. Miller.

**Resources:** Youssef Jounaidi.

**Supervision:** Keith W. Miller.

**Writing – original draft:** Rooma Desai, Wojciech J. Stec, Youssef Jounaidi.

**Writing – review & editing:** Wojciech J. Stec, Keith W. Miller.

## References

1. Olsen RW, Sieghart W. GABA A receptors: subtypes provide diversity of function and pharmacology. *Neuropharmacology*. 2009; 56(1):141–8. <https://doi.org/10.1016/j.neuropharm.2008.07.045> PMID: 18760291
2. Farrant M, Nusser Z. Variations on an inhibitory theme: phasic and tonic activation of GABA(A) receptors. *Nat Rev Neurosci*. 2005; 6(3):215–29. <https://doi.org/10.1038/nrn1625> PMID: 15738957
3. Brickley SG, Mody I. Extrasynaptic GABA(A) receptors: their function in the CNS and implications for disease. *Neuron*. 2012; 73(1):23–34. <https://doi.org/10.1016/j.neuron.2011.12.012> PMID: 22243744

4. Sieghart W. Allosteric modulation of GABAA receptors via multiple drug-binding sites. *Advances in Pharmacology*. 2015; 72:53–96. <https://doi.org/10.1016/bs.apha.2014.10.002> PMID: 25600367
5. Forman SA, Miller KW. Mapping General Anesthetic Sites in Heteromeric gamma-Aminobutyric Acid Type A Receptors Reveals a Potential For Targeting Receptor Subtypes. *Anesth Analg*. 2016; 123(5):1263–73. <https://doi.org/10.1213/ANE.0000000000001368> PMID: 27167687
6. Jensen ML, Wafford KA, Brown AR, Belelli D, Lambert JJ, Mirza NR. A study of subunit selectivity, mechanism and site of action of the delta selective compound 2 (DS2) at human recombinant and rodent native GABA(A) receptors. *Br J Pharmacol*. 2013; 168(5):1118–32. <https://doi.org/10.1111/bph.12001> PMID: 23061935
7. Hartiadi LY, Ahring PK, Chebib M, Absalom NL. High and low GABA sensitivity alpha4beta2delta GABAA receptors are expressed in *Xenopus laevis* oocytes with divergent stoichiometries. *Biochem Pharmacol*. 2016; 103:98–108. <https://doi.org/10.1016/j.bcp.2015.12.021> PMID: 26774457
8. Wongsamitkul N, Baur R, Sigel E. Toward Understanding Functional Properties and Subunit Arrangement of alpha4beta2delta gamma-Aminobutyric Acid, Type A (GABAA) Receptors. *J Biol Chem*. 2016; 291(35):18474–83. <https://doi.org/10.1074/jbc.M116.738906> PMID: 27382064
9. Eaton MM, Bracamontes J, Shu HJ, Li P, Mennerick S, Steinbach JH, et al. Gamma-aminobutyric acid type A alpha4, beta2, and delta subunits assemble to produce more than one functionally distinct receptor type. *Mol Pharmacol*. 2014; 86(6):647–56. <https://doi.org/10.1124/mol.114.094813> PMID: 25238745
10. Botzolakis EJ, Gurba KN, Lagrange AH, Feng HJ, Stanic AK, Hu N, et al. Comparison of gamma-Aminobutyric Acid, Type A (GABAA), Receptor alphabeta3 and alphabeta2 Expression Using Flow Cytometry and Electrophysiology: evidence for alternative subunit stoichiometries and arrangements. *J Biol Chem*. 2016; 291(39):20440–61. <https://doi.org/10.1074/jbc.M115.698860> PMID: 27493204
11. Wagoner KR, Czajkowski C. Stoichiometry of expressed alpha(4)beta(2)delta gamma-aminobutyric acid type A receptors depends on the ratio of subunit cDNA transfected. *J Biol Chem*. 2010; 285(19):14187–94. <https://doi.org/10.1074/jbc.M110.104257> PMID: 20233712
12. Dostalova Z, Liu A, Zhou X, Farmer SL, Krenzel ES, Arevalo E, et al. High-level expression and purification of Cys-loop ligand-gated ion channels in a tetracycline-inducible stable mammalian cell line: GABAA and serotonin receptors. *Protein Sci*. 2010; 19(9):1728–38. <https://doi.org/10.1002/pro.456> PMID: 20662008
13. Dostalova Z, Zhou X, Liu A, Zhang X, Zhang Y, Desai R, et al. Human alpha1beta3gamma2L gamma-aminobutyric acid type A receptors: High-level production and purification in a functional state. *Protein Sci*. 2014; 23(2):157–66. <https://doi.org/10.1002/pro.2401> PMID: 24288268
14. Reeves PJ, Callewaert N, Contreras R, Khorana HG. Structure and function in rhodopsin: high-level expression of rhodopsin with restricted and homogeneous N-glycosylation by a tetracycline-inducible N-acetylglucosaminyltransferase I-negative HEK293S stable mammalian cell line. *Proc Natl Acad Sci U S A*. 2002; 99(21):13419–24. <https://doi.org/10.1073/pnas.212519299> PMID: 12370423
15. Petersen TN, Brunak S, von Heijne G, Nielsen H. SignalP 4.0: discriminating signal peptides from transmembrane regions. *Nat Methods*. 2011; 8(10):785–6. <https://doi.org/10.1038/nmeth.1701> PMID: 21959131
16. Reeves PJ, Kim JM, Khorana HG. Structure and function in rhodopsin: a tetracycline-inducible system in stable mammalian cell lines for high-level expression of opsin mutants. *Proc Natl Acad Sci U S A*. 2002; 99(21):13413–8. <https://doi.org/10.1073/pnas.212519199> PMID: 12370422
17. Forman SA. A hydrophobic photolabel inhibits nicotinic acetylcholine receptors via open-channel block following a slow step. *Biochemistry*. 1999; 38(44):14559–64. PMID: 10545178
18. Lee HJ, Absalom NL, Hanrahan JR, van Nieuwenhuijzen P, Ahring PK, Chebib M. A pharmacological characterization of GABA, THIP and DS2 at binary alpha4beta3 and beta3delta receptors: GABA activates beta3delta receptors via the beta3(+)/delta(-) interface. *Brain Res*. 2016; 1644:222–30. <https://doi.org/10.1016/j.brainres.2016.05.019> PMID: 27181518
19. Adkins CE, Pillai GV, Kerby J, Bonnert TP, Haldon C, McKernan RM, et al. alpha4beta3delta GABA(A) receptors characterized by fluorescence resonance energy transfer-derived measurements of membrane potential. *J Biol Chem*. 2001; 276(42):38934–9. <https://doi.org/10.1074/jbc.M104318200> PMID: 11495904
20. Feng HJ, Bianchi MT, Macdonald RL. Pentobarbital differentially modulates alpha1beta3delta and alpha1beta3gamma2L GABAA receptor currents. *Mol Pharmacol*. 2004; 66(4):988–1003. <https://doi.org/10.1124/mol.104.002543> PMID: 15247320
21. Akk G, Bracamontes J, Steinbach JH. Activation of GABA(A) receptors containing the alpha4 subunit by GABA and pentobarbital. *J Physiol*. 2004; 556(Pt 2):387–99. <https://doi.org/10.1113/jphysiol.2003.058230> PMID: 14966300

22. Brown N, Kerby J, Bonnert TP, Whiting PJ, Wafford KA. Pharmacological characterization of a novel cell line expressing human  $\alpha(4)\beta(3)\delta$  GABA(A) receptors. *Br J Pharmacol*. 2002; 136(7):965–74. <https://doi.org/10.1038/sj.bjp.0704795> PMID: 12145096
23. Fisher JL, Macdonald RL. Single channel properties of recombinant GABAA receptors containing gamma 2 or delta subtypes expressed with alpha 1 and beta 3 subtypes in mouse L929 cells. *J Physiol*. 1997; 505 (Pt 2):283–97.
24. Liu K, Jounaidi Y, Forman SA, Feng HJ. Etomidate uniquely modulates the desensitization of recombinant  $\alpha 1\beta 3\delta$  GABA(A) receptors. *Neuroscience*. 2015; 300:307–13. <https://doi.org/10.1016/j.neuroscience.2015.05.051> PMID: 26028470
25. Tang X, Hernandez CC, Macdonald RL. Modulation of Spontaneous and GABA-Evoked Tonic  $\alpha 4\beta 3\delta$  and  $\alpha 4\beta 3\gamma 2L$  GABAA Receptor Currents by Protein Kinase A. *J Neurophysiol*. 2010; 103:1007–19. <https://doi.org/10.1152/jn.00801.2009> PMID: 19939957
26. Chiara DC, Dostalova Z, Jayakar SS, Zhou X, Miller KW, Cohen JB. Mapping general anesthetic binding site(s) in human  $\alpha 1\beta 3$  gamma-aminobutyric acid type A receptors with [(3)H]TDBzl-etomidate, a photoreactive etomidate analogue. *Biochemistry*. 2012; 51(4):836–47. <https://doi.org/10.1021/bi201772m> PMID: 22243422
27. Quirk K, Whiting PJ, Ragan CI, McKernan RM. Characterisation of delta-subunit containing GABAA receptors from rat brain. *Eur J Pharmacol*. 1995; 290(3):175–81. PMID: 7589211
28. Chiara DC, Jounaidi Y, Zhou X, Savechenkov PY, Bruzik KS, Miller KW, et al. General Anesthetic Binding Sites in Human  $\alpha 4\beta 3\delta$  gamma-Aminobutyric Acid Type A Receptors (GABAARs). *J Biol Chem*. 2016; 291(51):26529–39. <https://doi.org/10.1074/jbc.M116.753335> PMID: 27821594
29. Miller PS, Aricescu AR. Crystal structure of a human GABAA receptor. *Nature*. 2014; 512:270–5. <https://doi.org/10.1038/nature13293> PMID: 24909990
30. Barrera NP, Betts J, You H, Henderson RM, Martin IL, Dunn SM, et al. Atomic force microscopy reveals the stoichiometry and subunit arrangement of the  $\alpha 4\beta 3\delta$  GABA(A) receptor. *Mol Pharmacol*. 2008; 73(3):960–7. <https://doi.org/10.1124/mol.107.042481> PMID: 18079275
31. Hassaine G, Deluz C, Grasso L, Wyss R, Tol MB, Hovius R, et al. X-ray structure of the mouse serotonin 5-HT<sub>3</sub> receptor. *Nature*. 2014; 512(7514):276–81. <https://doi.org/10.1038/nature13552> PMID: 25119048
32. Kaur KH, Baur R, Sigel E. Unanticipated structural and functional properties of delta-subunit-containing GABAA receptors. *J Biol Chem*. 2009; 284(12):7889–96. <https://doi.org/10.1074/jbc.M806484200> PMID: 19141615
33. Meera P, Olsen RW, Otis TS, Wallner M. Alcohol- and alcohol antagonist-sensitive human GABAA receptors: tracking delta subunit incorporation into functional receptors. *Mol Pharmacol*. 2010; 78(5):918–24. <https://doi.org/10.1124/mol.109.062687> PMID: 20699325
34. Zhang Y, Jounaidi Y, Sarver LS, Zhou XJ, Cafiso DS, Miller KW.  $\gamma$ -Aminobutyric acid induced conformational change in GABAAR measured by pulsed electron paramagnetic resonance. *Biophys J*. 2014; 106(2):547a.